

Original Article

Entropy Weighted TOPSIS Taguchi Analysis of Notch Geometry on the Fatigue Performance of UNS S32760 Grade Stainless Steel

Jagadesh Kumar Jatavallabhula^{1*}, Vaddi Venkata Satyanarayana², Vasudeva Rao Veeredhi¹

¹Department of Mechanical, Bioresources and Biomedical Engineering,
College of Science, Engineering and Technology, University of South Africa, Florida Campus, Johannesburg, South Africa.
²Department of Mechanical Engineering, Vidya Jyothi Institute of Technology, Telangana, India.

*Corresponding Author : jagadeshkumar82@gmail.com

Received: 12 April 2024

Revised: 22 May 2024

Accepted: 12 June 2024

Published: 30 June 2024

Abstract - In the current research, the effect of notch geometric properties on the fatigue response of UNS S32760 steel is investigated. V-Notches with different notch parameters are prepared on the specimens, and the “fatigue life” of notched specimens is compared to that of the unnotched counterpart by undertaking strain-controlled fatigue experimental runs. The “fall in fatigue life” and the “fatigue notch factor” (from FEM) are also recorded for all the specimens. Entropy-weighted TOPSIS-Taguchi analysis is carried out on the L9 orthogonal array undertaken to quantify the effect of notch geometric parameters on the fatigue performance of the chosen material. It was found that the fatigue life of the un-notched coupon was 26016 cycles under the strain-controlled fatigue test condition applied. When V-notches of different geometries were made on the coupons, the fatigue life had fallen to a least 620 cycles (Run 3), amounting to a 97% reduction when the width, depth and central angle of the notch are 1 mm, 1 mm and 360° respectively. The contribution of the depth of the notch was 34.58%, the central angle was 24.14%, and the width of the notch governed to the extent of 16.32% on the overall output responses of fatigue life, fall in fatigue life and fatigue notch factor.

Keywords - Entropy weight, Taguchi method, Orthogonal array, Fatigue life, Fatigue notch factor.

1. Introduction

Fatigue failure occurs in materials due to repeated stresses, finally resulting in fracture under a stress level significantly lesser than that is essential to cause failure under monotonic loading conditions [1]. Fatigue failure in most of the engineering components commonly initiates at notches. Notch fatigue analysis gained prominence in the field of metal fatigue due to its high impact on the life of a component. Several theories like “Theory of critical distance”, “Local stress-strain approach”, “Nominal stress approaches”, “Weighting parameters-based approaches”, etc., were developed for quantifying the effect of notches on the fatigue life of engineering components [2, 3]. The theoretical stress concentration factor (Kt) and the fatigue notch factor (Kf), which are widely employed in notch fatigue life prediction, are parameters that arise from the existence of notches. Furthermore, when the component is subjected to tensile mean stress, the existence of notches may result in a decrease in fatigue life, but the presence of mean compressive stress typically results in an improvement in fatigue life. Consequently, the fatigue life of materials is greatly impacted by the presence of notches, especially in the automotive

industry [4]. When forecasting a component's fatigue life, the notch effect is crucial. Inhomogeneous stress fields produced by geometric feature-induced stress concentrations tend to cause crack sprouting and, ultimately, fracture failure [5]. Investigating the notch effect on fatigue behavior contributes to the formulation of analytical methods for designing notched specimens and performing numerical simulations to assess their behavior. Studying the notch effect in very high-cycle fatigue behaviour is important in improving fatigue assessment, understanding fatigue limit regimes, and enhancing the reliability and durability of engineering structures and components [6]. A novel structural stress approach for computing the effect of notch on fatigue life was developed, and it was found to be more effective than the stress-based methods [7]. Few researchers attempted to perform fatigue analysis of metals and alloys using statistical approaches [8, 9]. Taguchi technique is a statistical optimization method that aids in forecasting the optimal parameter conditions that can maximize/ minimize the response variable depending on the type of response variable [10]. The primary goal of TOPSIS is an estimation of the best replacements by minimizing the distance to the positive (+ve)



ideal solution and maximizing the distance to the negative (-ve) ideal solution [11]. The TOPSIS Taguchi analysis is a suitable technique for multi-response optimization studies as it is simple and easily adaptable when compared to other multi-attribute decision making Taguchi techniques like Grey Relational Analysis and VIKOR. These techniques can become extremely complex with an increase in the number of responses [12]. The entropy method estimates the ‘weights’ of attributes relying on the corresponding values of the objective. If an attribute has higher prominence over the others, its entropy value will be smaller, i.e. it epitomizes a heavyweight.

In short, the “Entropy Weight Method” was used to compute the “Relative Weights” of the response variables [13]. When it comes to single output optimization, the Taguchi method is the best fit at the least cost. However, in real time engineering scenarios, having a single output to optimize is generally rare, and there would be several responses that need to be optimized. TOPSIS method enables multiple responses to be prioritized by mathematically measuring the Euclidean distance from the ideal solutions, and it is a tradeoff solution between inferior and superior results. Further, entropy weighting of responses helps in the segregation [14].

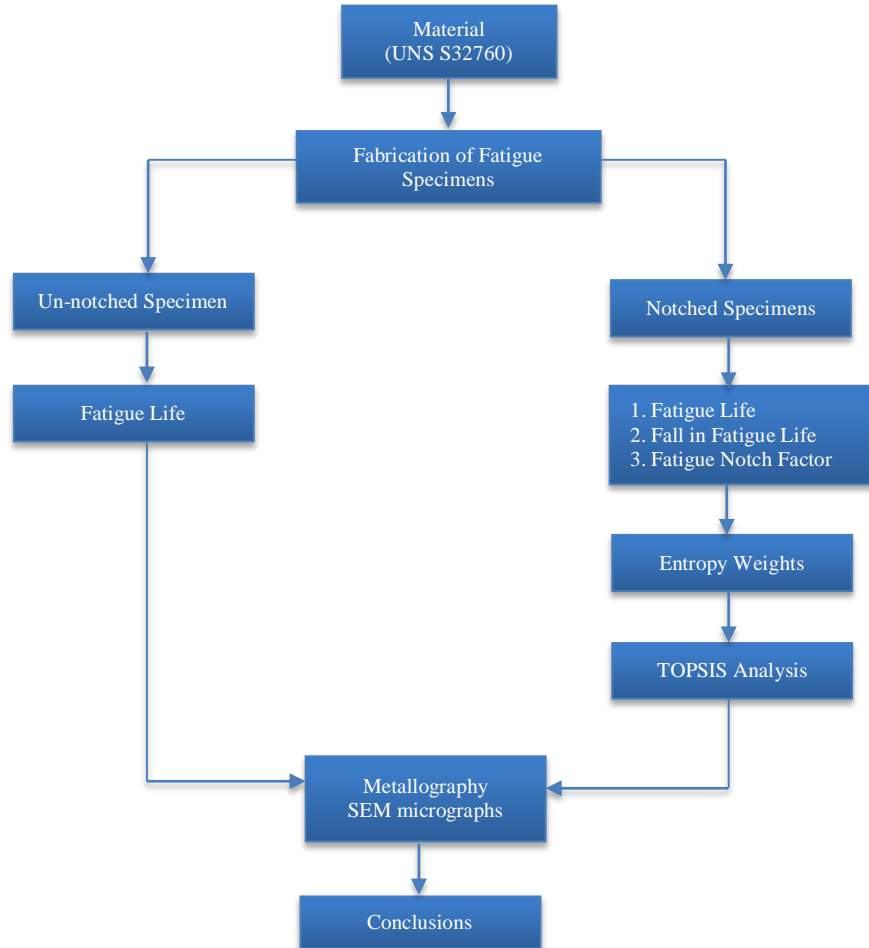


Fig. 1 Flowchart of the research work

In the current research, the effect of V-notch geometric properties on the fatigue response of UNS S32760 stainless steel is investigated. V-notches are undertaken as most of the grazes that get formed on engineering components upon usage are near the V-shape, and they have a more deteriorating effect on the life of components when compared to rectangular or U-notches. Notches with different geometric properties are prepared on the specimens and their “Fatigue lives” are compared to that of the unnotched counterpart by undertaking strain-controlled fatigue experimental runs. The “Fall in fatigue life” and the “Fatigue notch factor” are also recorded

for all the specimens. “Entropy weighted TOPSIS Taguchi Analysis” is carried out on the L9 orthogonal array to estimate the effect of notch geometric properties on the fatigue response of the chosen material. The fatigue life was the primary response that was intended to be evaluated in the current research, but during the investigation the vitality of fall in fatigue life and the fatigue notch factor were also appreciated. Hence, the three responses viz. “FL”, “FFL”, and “FNF” are undertaken as the responses. The priority of these responses, however, is a fuzzy notion, and it varies from one investigator to another. Hence, it was decided to employ the

entropy-weighted TOPSIS Taguchi technique for the optimization of the responses so that priorities would be scientifically established. Literature is scarce in the area of notch fatigue analysis using statistical approaches, and there is clearly a good scope for further research. Current research is inspired by the available research gap in the area of notch fatigue analysis using statistical methods. A novel approach to analyzing the factors; “FL” and “FFL” from experimental results and “FNF” from finite element results is adopted. The research work carried out is illustrated as a flowchart in Figure 1.

2. Materials and Methods

2.1. Material

UNS S32760 is a popular marine-grade super duplex stainless steel, and the same is considered for the current work due to its prevalent usage in components which are prone to fatigue loading [12].

The chemical composition (wt%) is presented in Table 1, while Table 2 tabulates the mechanical properties of the chosen material.

Table 1. Chemical composition (wt %)

Element	C	Si	Mn	P	S	Cr
Catalog	Max 0.030	0.10 – 0.80	Max 1.00	Max 0.025	Max 0.005	24.00 – 26.00
Actual	0.018	0.296	0.572	0.021	0.001	24.087
Element	Mo	Ni	N	W	Cu	Fe
Catalog	3.00 – 4.00	6.00 – 8.00	0.20 – 0.30	0.50 – 1.00	0.50 – 1.00	Bal
Actual	3.931	7.394	0.273	0.509	0.629	Bal

Table 2. Mechanical properties

Property	Catalog	Actual
Modulus of Elasticity (GPa)	190 – 201	200
Poisson's Ratio	0.3	0.3
Brinell Hardness (HBW)	Max 270	201
Tensile Strength (MPa)	730 – 930	898

2.2. Fatigue Specimen

The chosen stainless steel possesses high compositions of chromium and nickel that provide superior corrosion resistance, and hence, it is used popularly in marine components. The sea tidal waves cause low cycle fatigue on the components, and hence, it is necessary to study the fatigue behaviour under various crack conditions.

In this pursuit, cracks are artificially prepared in the form of notches on the specimens in the present investigation. The fatigue specimens were prepared as specified by the ASTM E606 standard on CNC lathe and CNC milling machines.

The specimen drawing is shown in Figure 2, along with a pictorial representation of the V-notch parameters, i.e. width of notch (w), depth of notch (d) and notch central angle (a).

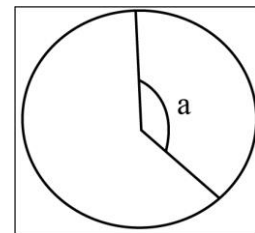
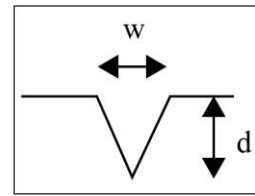
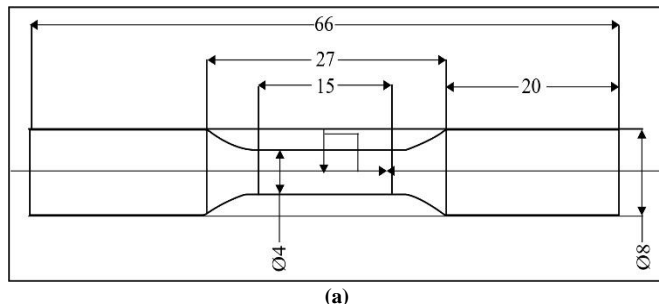


Fig. 2 Specimen and Notch geometric properties, (a) Fatigue specimen as per E606 standard, (b) Width and Depth of the V-notch, and (c) Central angle of the notch,

The specimens post-fabrication are shown in Figure 3.



Fig. 3 Un-notched (top) and notched (1-9 below) fatigue specimens

2.3. Fatigue Testing Machine

Fatigue experimentation was carried out on a 25kN Nano UTM (Make: ITW – BISS) with Servo Hydraulic control. It is a computer-controlled machine with fatigue accessories, extensometers and a data acquisition system. The machine supports total stress-control and total strain-control fatigue testing methodologies. Total strain control fatigue experimental runs are carried out at room temperature in the current research at a strain amplitude of 0.3%.

2.4. Finite Element Fatigue Analysis

In strain-controlled fatigue experimentation, the stress varies at every fraction of a second, and hence, the Fatigue Notch Factor cannot be directly computed from experimental results. The “fatigue notch factor” was arrived at through the finite element method, employing the ANSYS 18.1 fatigue tool. Analysis was carried out for the un-notched specimen and the nine notched counterparts with different types of notch geometric properties.

2.4.1. Boundary Conditions

The boundary conditions comprise a fixed support on one side and a pressure on the other side of the specimen. The induced stress was noted from ANSYS output. From the iterative approach, it was known that, for a pressure of 80MPa, maximum induced stress was very much lower than the endurance limit of the material, and the un-notched specimen thus possessed an infinite life under fatigue loading ($>10^6$). The un-notched and notched specimens were hence provided with a fixed support on the left side and a pressure of 80MPa on the right side in the direction, as shown in Figure 4.

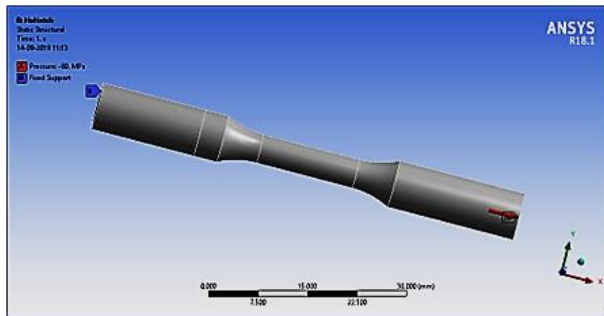


Fig. 4 Boundary conditions applied in FEM

“Von-Mises stress” and “Fatigue life” were recorded from ANSYS output. “Fatigue notch factor” was computed from the ratio of stress induced in the notched specimen to the stress induced in the un-notched specimen.

2.5. Design of Experiments

2.5.1. Notch Parameters/ Factors

Notches of three varied geometric parameters, i.e. “width”, “depth”, and “notch central angle”, are prepared on the fatigue specimens. Table 3 tabulates the factors selected at three levels in the current research. Taguchi L_9 orthogonal array, as shown in Table 4, was chosen for current research in

combination with entropy weighted TOPSIS method for the analysis.

Table 3. Selected factors with their levels

Factor	Units	Notation	Levels		
			Low	Medium	High
Width	mm	w	1	1.25	1.5
Depth	mm	d	0.5	0.75	1
Notch Central Angle	degree	a	120°	240°	360°

Table 4. Taguchi L_9 array

Run	Width (mm)	Depth (mm)	Notch Central Angle
1	1	0.5	120°
2	1	0.75	240°
3	1	1	360°
4	1.25	0.5	240°
5	1.25	0.75	360°
6	1.25	1	120°
7	1.5	0.5	360°
8	1.5	0.75	120°
9	1.5	1	240°

2.5.2. Response Variables

The “fatigue life”, “fall in fatigue life”, and the “fatigue notch factor” were chosen as the response variables. The objective was to maximize the fatigue life and to minimize the fall in fatigue life and fatigue notch factor. Fall-in fatigue life for a notched specimen is the difference between the fatigue life of an un-notched specimen and the notched specimen under consideration. “Fatigue Notch Factor” for a specimen was computed from the ratio of stresses induced in the notched and un-notched specimen under consideration (from FEM analysis).

2.6. Entropy-Weighted TOPSIS Method

TOPSIS was originally conceptualized in the year 1981 by Hwang and Yoon. Best alternatives are discovered in TOPSIS by minimizing the distance w.r.t. the positive ideal solution and maximizing the distance w.r.t. the negative-ideal solution [15]. Different solutions may be ranked as per their nearness to the ideal solution. The entropy-weighted method was originally developed by Shannon and Weaver in 1947. Later, Zeleny extended the method in 1982. It is used to assign the objective weights of the attributes/ responses. The probability approach is applied to calculate indeterminate information, which is termed entropy. The entropy-weighted method relies on the volume of information to compute the weight of the response variable and is one of the objective weight methods [16]. In the current research, Entropy weighted TOPSIS method is taken up as an optimization algorithm, and the method is depicted as a flowchart in Figure 5.

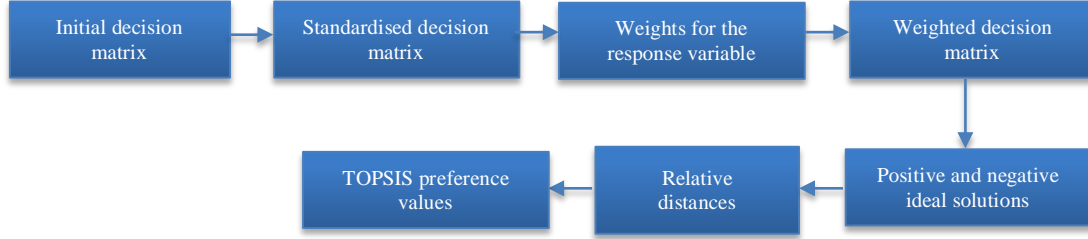


Fig. 5 Entropy weighted TOPSIS taguchi method

The initial decision matrix for ‘n’ response variables, with each variable having ‘m’ alternative values, will be represented by matrix A as given in Equation (1).

$$A = \begin{bmatrix} a_{11} & a_{12} & \dots & a_{1n} \\ a_{21} & a_{22} & \dots & a_{2n} \\ a_{31} & a_{32} & \dots & a_{3n} \\ \vdots & \vdots & \vdots & \vdots \\ a_{m1} & a_{m2} & \dots & a_{mn} \end{bmatrix} \quad (1)$$

The “standardized decision matrices” are obtained with an objective to maximize the fatigue life and minimize the fall in fatigue life and the fatigue notch factor using Equation (2) to (4);

$$r'_{ij} = \frac{a_{ij}}{\max(a_{ij})}, i = 1, 2, 3, \dots, m; j = 1, 2, 3, \dots, n \quad (2)$$

$$r''_{ij} = \frac{\min(a_{ij})}{a_{ij}}, i = 1, 2, 3, \dots, m; j = 1, 2, 3, \dots, n \quad (3)$$

$$r_{ij} = \frac{r'_{ij}}{\sum_{i=1}^m r'_{ij}}, i = 1, 2, 3, \dots, m; j = 1, 2, 3, \dots, n \quad (4)$$

The “standardized decision matrices” are found using the relation $R = (r_{ij})_{m \times n}$. The weights of the response variables at various conditions were computed by means of the entropy method. The term e_j represents the entropy of the j^{th} response in the standardized decision matrix, and ‘E’ signifies the total entropy of the responses.

The term d_j represents dispersity and w_j represents the weights of the responses. The summation of the weights of response variables should be unity. The Equations (5) - (9) have been employed to compute entropy, dispersity and weights for the response under consideration.

$$e_j = -k \sum_{i=1}^m r_{ij} \ln r_{ij}, j = 1, 2, 3, \dots, n \quad (5)$$

$$k = \frac{1}{\ln m} \quad (6)$$

$$E = \sum_{j=1}^n e_j = \frac{-1}{\ln m} \sum_{j=1}^n \sum_{i=1}^m r_{ij} \ln r_{ij} \quad (7)$$

The dispersity of variable j was found using Equation (8);

$$d_j = 1 - e_j; j = 1, 2, 3, \dots, n \quad (8)$$

The weight factor was computed using Equation (9);

$$w_j = \frac{d_j}{\sum_{j=1}^n d_j} \quad (9)$$

3. Results and Discussion

“Fatigue Life” and the “Fall in Fatigue Life” were experimentally found by undertaking experiments on the specimens as per ASTM E606 standard for strain-controlled fatigue testing. In order to maintain the predetermined strain amplitude, the stress varies continuously during the experimental run.

The initial magnitude of stress would be highest, and as the fatigue cycles progress, the stress levels would decrease, indicating the reduction in strength of the material due to the setting up of the slip phenomenon. The energy absorbed by the material gets reduced as the cycles progress and this eventually leads to early failure.

As mentioned in section 2.4, the “Fatigue Notch Factor” was computed using Finite Element Method (FEM). The value of the ‘Fatigue Notch Factor’ was taken as the ratio of stress induced in the notched specimen under consideration and that of the un-notched specimen. The computation method of fatigue notch factor for a typical specimen (Run 9) is furnished as an example. Figures 6 and 7 show the contour plots of the stress induced in the un-notched specimen and the notched specimen of Run 9 for the applied boundary conditions, respectively.

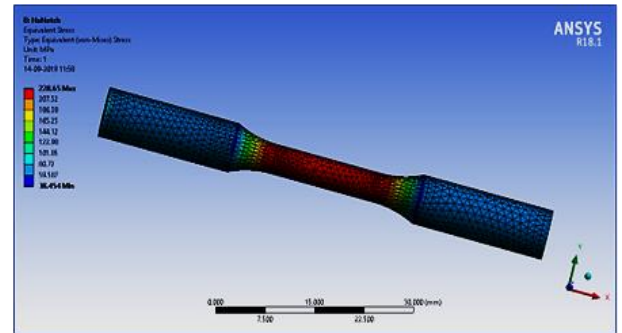


Fig. 6 Stress induced in un-notched specimen

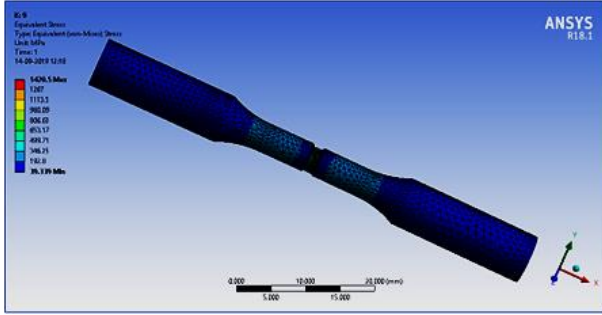


Fig. 7 Stress-induced in notched specimen – run 9

Due to the applied boundary conditions, the stress induced in the un-notched specimen is 228.65 MPa (Figure 6), while the stress induced in a typical notched specimen of Run 9 is 1420.5 MPa (Figure 7). Hence the “Fatigue Notch Factor” for it is found by taking the ratio of those stresses, i.e. $1420.5/228.65 = 6.21$. It is computed similarly for all the other specimens. ‘Fall in Fatigue Life’ was computed by subtracting the life of each of the notched specimens from the “Fatigue Life” of the un-notched specimen. The fatigue tests were conducted two to three times per scenario for the sake of consistency and accuracy, as specified in the ASTM E606 standard. The mean of the test results is tabulated for the un-notched specimen in Table 5.

Table 5. Fatigue life of un-notched UNS S32760 steel

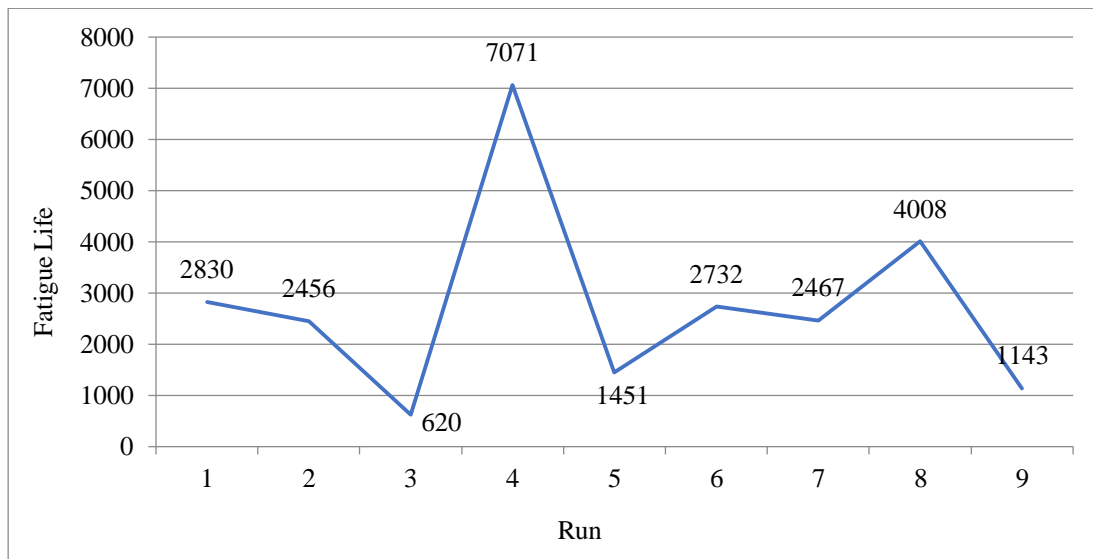
Specimen Type	Fatigue Life (Cycles)
Un-notched	26016

The notches on the specimens are created by means of a CNC lathe and milling machines. Fatigue test results for the specimens with various geometric types of V-notches are tabulated in Table 6, and the trends are presented graphically in Figure 8. The fatigue life of the un-notched specimen was 26016 cycles, while it reduced abnormally to a range of 620-

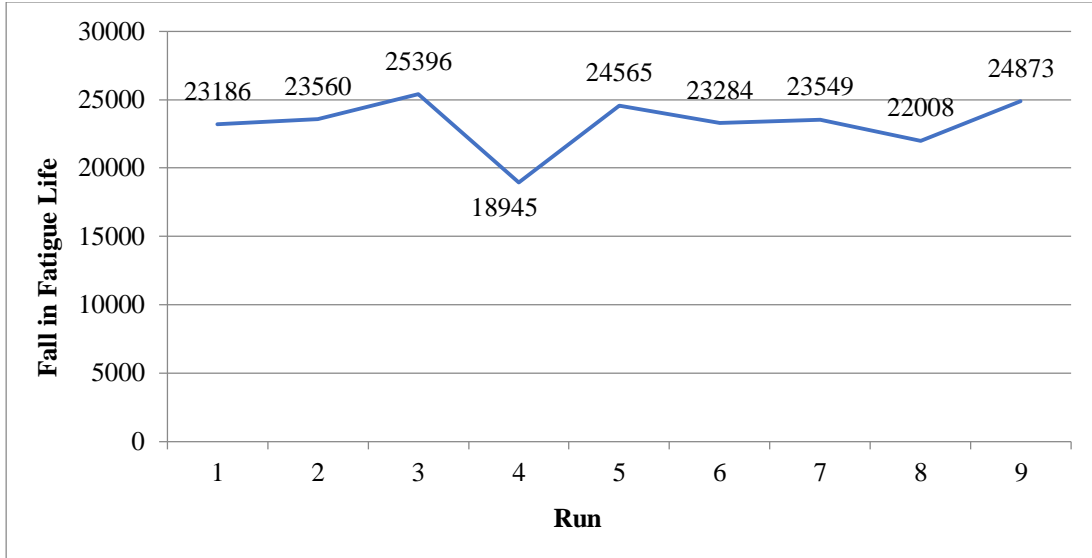
7071 cycles when notches were created on the specimens. The fatigue life variation depicted in Figure 8(a) manifests that the local minima occurred at four places with a magnitude of (620, 1461, 2467, 1143) cycles, while the local maxima occurred with a magnitude of (2830, 7071, 2732, 4008) cycles. The local minima for fall in fatigue life and fatigue notch factor can be extracted from Figures 8(b) and 8(c) to identify and analyze further. When the depth of the notch increased, the fatigue notch factor also increased proportionately and led to a reduction in fatigue life. This can be attributed to the high-stress concentration at the groove due to the re-distribution of loading at the edge of the sharp notch that promoted the early failure. A single-point cutting tool with a nose radius of 0.25 mm was employed on the lathe machine, and a notch of width 1 mm, depth 1 mm and central angle of 360° was prepared on the fatigue specimen. The fatigue test was conducted on that specimen, and the fatigue life was found to be 1503 cycles, which is higher than the specimen without a radius at the root of the notch. The stress concentration was reduced with the elimination of sharp edge at the root and that resulted in the improvement of fatigue life.

Table 6. Experimental and FEM results

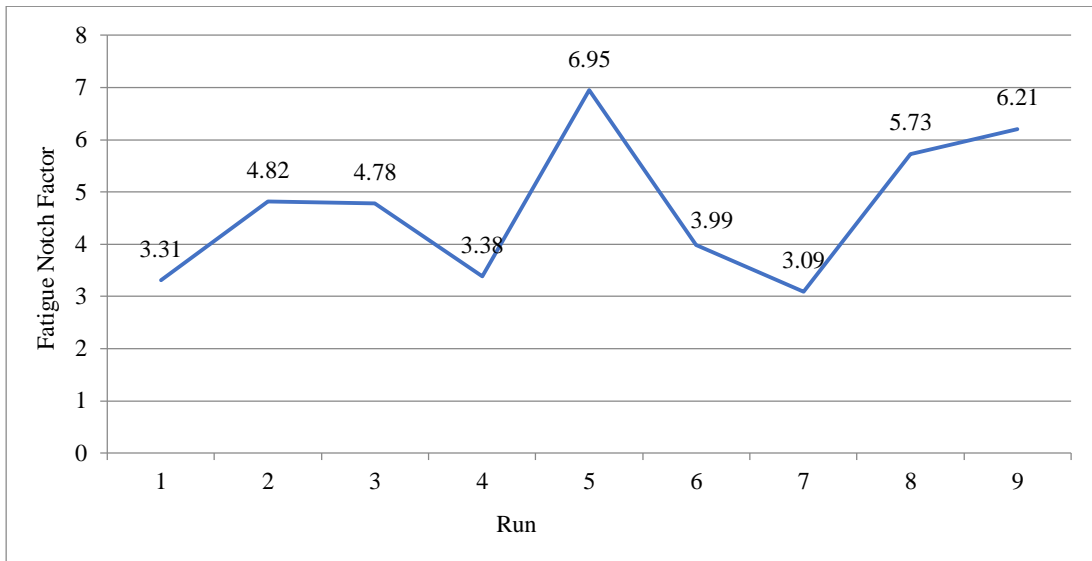
Run	Width (mm)	Depth (mm)	Notch Central Angle	FL	FFL	FNF
1	1	0.5	120°	2830	23186	3.31
2	1	0.75	240°	2456	23560	4.82
3	1	1	360°	620	25396	4.78
4	1.25	0.5	240°	7071	18945	3.38
5	1.25	0.75	360°	1451	24565	6.95
6	1.25	1	120°	2732	23284	3.99
7	1.5	0.5	360°	2467	23549	3.09
8	1.5	0.75	120°	4008	22008	5.73
9	1.5	1	240°	1143	24873	6.21



(a)



(b)

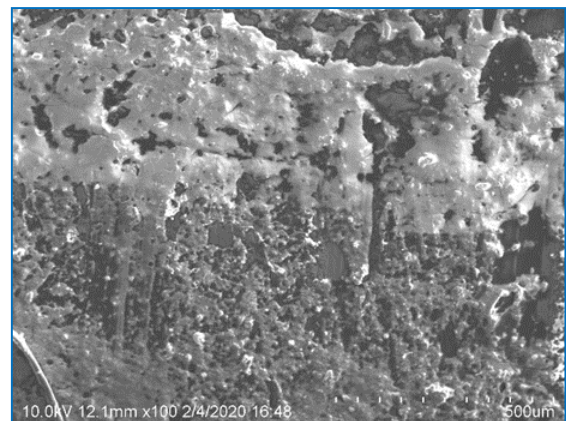


(c)

Fig. 8 Trends of the responses chosen,
(a) Fatigue life, (b) Fall in fatigue life, and (c) Fatigue notch factor.

The un-notched specimen absorbed more energy when compared to the notched counterparts and hence it yielded higher fatigue life. Fractography was performed using a Scanning Electron Microscope to understand the type of failure that occurred for un-notched and notched specimens.

Figure 9(a) shows the SEM image of an un-notched specimen displaying a more simple structure, indicating a ductile fracture, while Figure 9(b) is the SEM image of a notched specimen displaying a kind of cleavage fracture owing to crack propagation across grain boundary. The artificial cracks created in the form of notches shoot up the stresses at the root, and multiple slip systems are created along the grain boundaries, which eventually propagate the cracks.



(a)

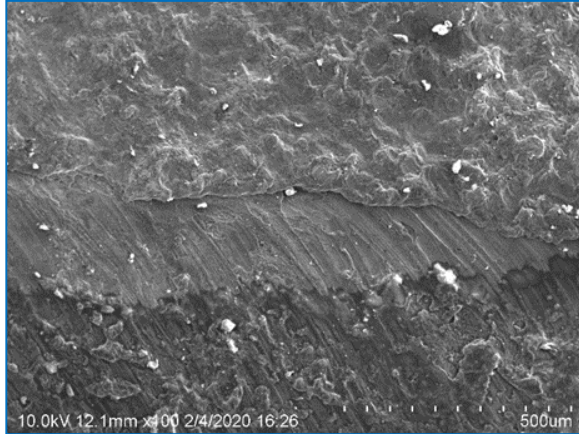


Fig. 9 Scanning electron microscopic images a) Un-notched specimen, and b) Notched specimen.

The normalization of the output parameters was carried out; the higher, the better criterion was employed for fatigue life, while the lower, the better was attributed to fall in fatigue life and fatigue notch factor. The fatigue life of each of the runs was divided by the maximum fatigue life in the domain for a normalized value of fatigue life, while a ratio between the minimum value in the domain to each of the run values was undertaken for a fall in fatigue life and fatigue notch factor. The normalized values of the output responses are tabulated in Table 7.

Table 7. Normalized results of the responses

Run	FL	FFL	FNF
1	0.4002	0.8171	0.9335
2	0.3473	0.8041	0.6411
3	0.0877	0.7460	0.6464
4	1.0000	1.0000	0.9142
5	0.2052	0.7712	0.4446
6	0.3864	0.8136	0.7744
7	0.3489	0.8045	1.0000
8	0.5668	0.8608	0.5393
9	0.1616	0.7617	0.4976

Table 8. Standardized results of the responses (S_{ij})

Run	FL	FFL	FNF
1	0.1142	0.1107	0.1461
2	0.0991	0.1090	0.1003
3	0.0250	0.1011	0.1011
4	0.2854	0.1355	0.1430
5	0.0586	0.1045	0.0696
6	0.1103	0.1103	0.1212
7	0.0996	0.1090	0.1565
8	0.1618	0.1167	0.0844
9	0.0461	0.1032	0.0779

The normalized output parameters are converted to a standardized format relative to the respective mean of each of the responses by taking a ratio between each of the run values

to aggregate the corresponding response. The standardized results are presented in Table 8. Equations (2)-(4) were employed to transform the output responses into normalized and standardized results.

The standardized results were processed for computation of entropy and dispersity using Equations (5)-(9). The entropies of the responses manifest the weights to be given to the respective output parameter. The larger weight indicator divulges more constructive information than the lower weight indicator for any given response parameter under consideration.

The dispersity is the magnitude of the probability of the divergence in the form of lower weight allocated to a response. The entropy, dispersity and weights of the responses computed are presented in Table 9. The weighted results of the responses were computed as the product of weight and standardized results, i.e. $\sum_{i=1, j=1}^{i=m, j=n} w_j S_{ij}$ they are compiled in Table 10.

Table 9. Weights of the responses

--	FL	FFL	FNF
Entropy	0.9114	0.9983	0.9832
Dispersity	0.0886	0.0017	0.0168
Weight (w_{ij})	0.8276	0.0155	0.1569

Table 10. Weighted results of the responses

Run	FL	FFL	FNF
1	0.09453	0.00171	0.02292
2	0.08204	0.00169	0.01574
3	0.02071	0.00156	0.01587
4	0.23618	0.00210	0.02244
5	0.04847	0.00162	0.01092
6	0.09125	0.00171	0.01901
7	0.08240	0.00169	0.02455
8	0.13387	0.00180	0.01324
9	0.03818	0.00160	0.01222

Table 11. Ideal solutions and closeness coefficient

Run	Positive Ideal (L^+)	Negative Ideal (L^-)	Closeness Coefficient (CC)
1	0.142165099	0.073837186	0.341835209
2	0.154225179	0.061957023	0.286596319
3	0.215532508	0.008696176	0.038782619
4	0.011540959	0.215485834	0.949164769
5	0.187718583	0.030928846	0.141455336
6	0.145156863	0.070762865	0.327727649
7	0.154385602	0.061694636	0.285517253
8	0.102336638	0.113729823	0.526365002
9	0.19801063	0.021390622	0.097495443

Table 11 is furnished with “Positive Ideal Solution”, “Negative Ideal Solution”, and “Closeness Coefficient” computed as per TOPSIS methodology [17].

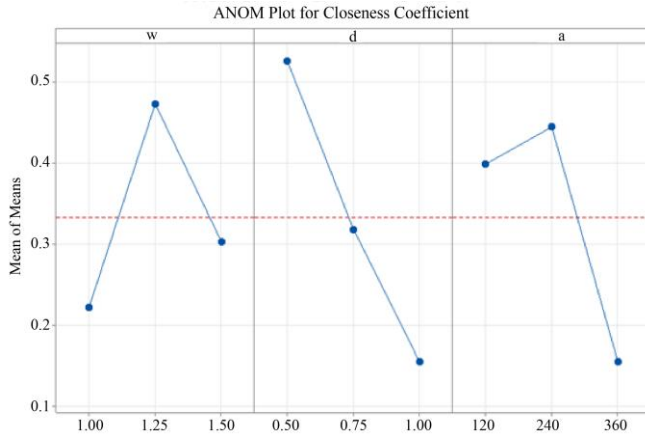


Fig. 10 ANOM plot for closeness coefficient

Table 12. Optimal parameter condition

Parameter	Optimal Condition	Units
w	1.25	mm
d	0.5	mm
a	240	degrees

ANOM and ANOVA were performed for the closeness coefficients as per Yate's algorithm [18]. The ANOM plot for the closeness coefficient is shown in Figure 10, and the optimal parameter condition for the overall multi-objective function is employed by using a higher the better criterion. Table 12 shows the optimal parameter condition to have a comprehensive solution.

A regression equation is generated from Taguchi analysis for the fatigue life (f), and it is represented by Equation (10) with the variables in coded form. It illustrates the quantum of fatigue life affected by individual parameters in their isolation. The depth of the notch takes a major role as it has a negative coefficient of 1312, while the angle of the notch plays a minor role in the fatigue life prediction.

$$f = 2753 + 285w - 1312d - 839a \quad (10)$$

The ANOVA of the closeness coefficient is tabulated in Table 13.

Table 13. ANOVA for the closeness coefficient

Source	DF	SS	MS	Contribution (%)
w	2	0.09799	0.04899	16.32
d	2	0.20724	0.10362	34.52
a	2	0.14495	0.07248	24.14
Error	2	0.15009	0.07505	--
Total	8	0.60028	--	--

The output responses are governed by the input parameters, i.e. width, depth and central angle in the range varying between 16.32 to 34.52%. The depth of the notch was the highest influencer (34.52%) in varying the fatigue output responses, while the width of the notch contributed to a tune

of 16.32%, as manifested by the regression equation. The optimal parameter condition arrived at in the present investigation matched with experimental results of Run 4. The optimal fatigue life was 7071 cycles, the fall in fatigue life was 18945 cycles, and the fatigue notch factor was 3.38.

4. Conclusion

- The fatigue life of un-notched UNS S32760 steel was 26016 cycles under strain-controlled fatigue test conditions applied.
- When V-notches of different geometries are made on the coupons, the fatigue life has fallen to a least 620 cycles (Run 3), amounting to a 97% reduction when the width, depth and central angle of the notch are 1 mm, 1 mm and 360° respectively.
- The fatigue life with a sharp root-edged notch has 620 cycles, while the life had increased to 1503 cycles when the root was filleted to a radius of 0.25 mm when the width and depth of the notch were 1 mm and central angle was 360°.
- The fracture in the fatigue test of the un-notched specimen was found to be ductile, while with a notch, it had cleavage and propagated through the grain boundary.
- The contribution of the depth of the notch was 34.52%, the central angle was 24.14%, and the width of the notch governed to the extent of 16.32% on the overall output responses of fatigue life, fall in fatigue life and fatigue notch factor.
- The optimal condition for the notch geometry was 1.25 mm width, 0.5 mm depth and 240° central angle, which had a fatigue life of 7071 cycles.

Acknowledgements

The authors thank the University of South Africa for providing an opportunity to undertake the current research as part of the postdoctoral research program. The authors also thank the Head of the Mechanical Engineering Department, Vidya Jyothi Institute of Technology, for the valuable suggestions given during the research work.

Abbreviations

FEM: Finite Element Method
 VIKOR: Vlekrerijumsko KOMPromisno Rangiranje
 TOPSIS: Technique for Order of Preference by Similarity to Ideal Solution
 ANOM: Analysis of Means
 ANOVA: Analysis of Variance
 UTM: Universal Testing Machine
 FL: Fatigue Life
 FFL: Fall in Fatigue Life
 FNF: Fatigue Notch Factor
 SS: Sum of Squares
 MS: Mean Squares
 DF: Degrees of Freedom

References

- [1] Ashutosh Sharma, Min Chul Oh, and Byungmin Ahn, "Recent Advances in Very High Cycle Fatigue Behavior of Metals and Alloys-A Review," *Metals*, vol. 10, no. 9, pp. 1-24, 2020. [[CrossRef](#)] [[Google Scholar](#)] [[Publisher Link](#)]
- [2] Wen-Long Ye et al., "Fatigue Life Prediction of Notched Components Under Size Effect Using Stress Gradient-Based Approach," *International Journal of Fracture*, vol. 234, pp. 249-261, 2022. [[CrossRef](#)] [[Google Scholar](#)] [[Publisher Link](#)]
- [3] Ding Liao et al., "Recent Advances on Notch Effects in Metal Fatigue: A Review," *Fatigue and Fracture of Engineering Materials and Structures*, vol. 43, no. 4, pp. 637-659, 2020. [[CrossRef](#)] [[Google Scholar](#)] [[Publisher Link](#)]
- [4] Surajit Kumar Paul, "Effect of Forming Strain on Low Cycle, High Cycle and Notch Fatigue Performance of Automotive Grade Dual Phase Steels: A Review," *Forces in Mechanics*, vol. 11, pp. 1-18, 2023. [[CrossRef](#)] [[Google Scholar](#)] [[Publisher Link](#)]
- [5] Muzhou Ma et al., "Fatigue Life Prediction for Notched Specimen Considering Modified Critical Plane Method," *Fatigue & Fracture of Engineering Materials and Structures*, vol. 46, no. 3, pp. 1031-1044, 2023. [[CrossRef](#)] [[Google Scholar](#)] [[Publisher Link](#)]
- [6] Rita Dantas et al., "Notch Effect in Very High-Cycle Fatigue Behaviour of a Structural Steel," *International Journal of Fatigue*, vol. 177, pp. 1-12, 2023. [[CrossRef](#)] [[Google Scholar](#)] [[Publisher Link](#)]
- [7] Yifei Yu et al., "A Structural Stress Approach Accounting for Notch Effects on Fatigue Propagation Life: Part I Theory," *International Journal of Fatigue*, vol. 159, 2022. [[CrossRef](#)] [[Google Scholar](#)] [[Publisher Link](#)]
- [8] K.V. Anderson, and S.R. Daniewicz, "Statistical Analysis of the Influence of Defects on Fatigue Life Using a Gumbel Distribution," *International Journal of Fatigue*, vol. 112, pp. 78-83, 2018. [[CrossRef](#)] [[Google Scholar](#)] [[Publisher Link](#)]
- [9] Andrea Tridello et al., "Statistical Models for Estimating the Fatigue Life, the Stress–Life Relation, and the P–S–N Curves of Metallic Materials in Very High Cycle Fatigue: A Review," *Fatigue and Fracture of Engineering Materials and Structures*, vol. 45, no. 2, pp. 332-370, 2022. [[CrossRef](#)] [[Google Scholar](#)] [[Publisher Link](#)]
- [10] B. Nagaraja et al., "Empirical Study for Nusselt Number Optimization for the Flow Using ANOVA and Taguchi Method," *Case Studies in Thermal Engineering*, vol. 50, pp. 1-17, 2023. [[CrossRef](#)] [[Google Scholar](#)] [[Publisher Link](#)]
- [11] Prabina Kumar Patnaik et al., "Multi-Objective Optimization and Experimental Analysis of Electro-Discharge Machining Parameters via Gray-Taguchi, TOPSIS-Taguchi and PSI-Taguchi Methods," *Materials Today: Proceedings*, vol. 62, no. 10, pp. 6189-6198, 2022. [[CrossRef](#)] [[Google Scholar](#)] [[Publisher Link](#)]
- [12] Bariş Şimşek, Yusuf Tansel İç, and Emir H. Şimşek, "A TOPSIS-Based Taguchi Optimization to Determine Optimal Mixture Proportions of the High Strength Self-Compacting Concrete," *Chemometrics and Intelligent Laboratory Systems*, vol. 125, pp. 18-32, 2013. [[CrossRef](#)] [[Google Scholar](#)] [[Publisher Link](#)]
- [13] Fei Lei et al., "Multiobjective Discrete Optimization Using the TOPSIS and Entropy Method for Protection of Pedestrian Lower Extremity," *Thin-Walled Structures*, vol. 152, 2020. [[CrossRef](#)] [[Google Scholar](#)] [[Publisher Link](#)]
- [14] Deepak Tiwari et al., "Parametric Optimization of Organic Rankine Cycle Using Topsis Integrated with Entropy Weight Method," *Energy Sources, Part A: Recovery, Utilization and Environmental Effects*, vol. 44, no. 1, pp. 2430-2447, 2022. [[CrossRef](#)] [[Google Scholar](#)] [[Publisher Link](#)]
- [15] Mohd Muqem et al., "Application of the Taguchi Based Entropy Weighted TOPSIS Method for Optimisation of Diesel Engine Performance and Emission Parameters," *International Journal of Heavy Vehicle Systems*, vol. 26, no. 1, pp. 69-94, 2019. [[CrossRef](#)] [[Google Scholar](#)] [[Publisher Link](#)]
- [16] Raman Kumar et al., "Revealing the Benefits of Entropy Weights Method for Multi-Objective Optimization in Machining Operations: A Critical Review," *Journal of Materials Research and Technology*, vol. 10, pp. 1471-1492, 2021. [[CrossRef](#)] [[Google Scholar](#)] [[Publisher Link](#)]
- [17] Yakup Çelikkilek, and Fatih Tüysüz, "An In-Depth Review of Theory of the TOPSIS Method: An Experimental Analysis," *Journal of Management Analytics*, vol. 7, no. 2, pp. 281-300, 2020. [[CrossRef](#)] [[Google Scholar](#)] [[Publisher Link](#)]
- [18] Douglas C. Montgomery, *Design and Analysis of Experiments*, 4th ed., Wiley, New York, pp. 1-704, 1997. [[Google Scholar](#)]